Quasi-static aberrations induced by laser guide stars in adaptive optics

Marcos A. van Dam
W. M. Keck Observatory, 65-1120 Mamalahoa Highway, Kamuela HI 96743
mvandam@keck.hawaii.edu

Antonin H. Bouchez
Caltech Optical Observatories, M/S 105-24, Pasadena, CA 91125

David Le Mignant and Peter L. Wizinowich
W. M. Keck Observatory, 65-1120 Mamalahoa Highway, Kamuela HI 96743

Abstract: Laser Guide Star Adaptive Optics (LGS AO) systems use the return from an artificial guide star to measure the wavefront aberrations in the direction of the science object. We observe quasi-static differences between the measured wavefront and the wavefront aberration of the science object. This paper quantifies and explains the source of the difference between the wavefronts measured using an LGS and a natural guide star at the W. M. Keck Observatory, which can be as high as 1000 nm RMS.

OCIS codes: (010.1080) Adaptive optics;(010.7350) Wave-front sensing.

References and links

1. D. L. Fried and J. F. Belsher, "Analysis of fundamental limits to artificial-guide-star adaptive-optics-system performance for astronomical imaging," J. Opt. Soc. Am A **11**, 277-287 (1994).
2. R. Ragazzoni, "Laser guide star advanced concepts: tilt problem," in *Laser Guide Star Adaptive Optics for Astronomy*, N. Ageorges and C. Dainty, eds. (Kluwer, Dordrecht, 1997), 125-146.
3. C. E. Max, "Laser guide star operational issues," in *Laser Guide Star Adaptive Optics for Astronomy*, N. Ageorges and C. Dainty, eds. (Kluwer, Dordrecht, 1997), 89-106.
4. P. L. Wizinowich, D. Le Mignant, A. H. Bouchez, R. D. Campbell, J. C. Y. Chin, A. R. Contos, M. A. van Dam, S. K. Hartman, E. M. Johansson, R. E. Lafon, H. Lewis, P. J. Stomski, D. M. Summers, C. G. Brown, P. M. Danforth and D. M. Pennington, "The W. M. Keck Observatory laser guide star adaptive optics system: overview," PASP **118**, 297-309 (2006).
5. M. A. van Dam, A. H. Bouchez, D. Le Mignant, R. D. Campbell, J. C. Y. Chin, S. K. Hartman, E. M. Johansson, R. Lafon, P. J. Stomski, Jr., D. M. Summers and P. L. Wizinowich, 'The W. M. Keck Observatory laser guide star adaptive optics system: performance characterization," PASP **118**, 310-318 (2006).
6. M. A. van Dam, D. Le Mignant and B. A. Macintosh, "Performance of the Keck Observatory adaptive-optics system," Applied Optics **43**, 5458-5467 (2004).
7. D. Summers, A. H. Bouchez, J. Chin, A. Contos, S. Hartman, E. Johansson, R. Lafon, D. Le Mignant, P. Stomski, M. A. van Dam and P. L. Wizinowich, "Focus and pointing adjustments necessary for laser guide star adaptive optics at the W.M. Keck Observatory," in *Advancements in Adaptive Optics*, D. Bonaccini Calia, B. L. Ellerbroek and R. Ragazzoni, eds, Proc. SPIE 5490, 1117-1128 (2004).
8. R. Ragazzoni, M. Tordi, and E. Diolati, "A fixed plate to remove spherical aberration in Rayleigh laser guide stars,", Opt. Comms. **194**, 243-250 (2001).
9. R. J. Noll, "Zernike polynomials and atmospheric turbulence," J. Opt. Soc. Am. **66**, 207-211 (1976).

1. Introduction

Adaptive Optics (AO) systems are now routinely used in astronomy to compensate for the time-varying wavefront aberrations caused by temperature gradients and turbulence in the Earth's

#68578 - $15.00 USD Received 2 March 2006; revised 11 April 2006; accepted 11 April 2006

atmosphere. One of the greatest limitations to AO is the need for a sufficiently bright wavefront reference close to the science object being studied. Sodium Laser Guide Star (LGS) AO systems overcome this limitation by creating an artificial guide star at an altitude of ~ 90 km at any location in the sky. When using an LGS AO system, the wavefront measured by the wavefront sensor (WFS) guiding on an LGS differs from the wavefront of light emanating from a natural guide star (NGS) as seen by the science camera. The differences are due to tip-tilt, focus, focal anisoplanatism, and other high-order effects which we will call "LGS aberrations".

It is well-known that atmospheric tip-tilt cannot be measured using an LGS, since the LGS is deflected equally on the upward and downward trajectory. Although many solutions have been proposed to avoid the need for an NGS to measure tip-tilt [2], none of them has yet been successfully implemented on an LGS AO system. In addition, there is a time-varying focus difference between the NGS and LGS due to the fact that a sodium LGS is located at a varying height centered at about 90 km and the NGS appears to be at an infinite height. In closed-loop operation, if the LGS is used to measure the wavefront then the focus of the science image changes as the mean height of the return from the LGS changes. This is compensated by changing the focal position of the wavefront.

Focal anisoplanatism arises because the light from the finite-altitude LGS samples a cone rather than a cylinder of turbulence above the telescope [1]. This limitation can be overcome only by projecting multiple LGSs. Higher-order aberrations induced by the apparent elongation of the LGS were predicted, and methods for compensating for them are presented in Ref. [3].

The remainder of this paper analyzes the high-order aberrations measured using the Keck II telescope's LGS AO system at the W. M. Keck Observatory. A full description of this system and its performance can be found in Refs. [4, 5, 6]. The Keck II LGS AO system uses a 589 nm wavelength laser, projected from a launch telescope located 6.2 m from the optical axis of the 10 m diameter telescope. To measure the LGS aberrations, as well as focus, a low-bandwidth wavefront sensor (LBWFS) guides on an NGS. A beamsplitter diverts 20% of the light of the NGS to the LBWFS, while the rest is sent to the fast tip-tilt sensor. Both the LBWFS and the fast wavefront sensor (WFS) guiding on the LGS are Shack-Hartmann sensors with 20×20 subapertures, and there is a one-to-one correspondence and registration between them. The WFS consists of quad cells (2×2 pixels per subaperture), so its centroid response is dependent on the elongation and orientation of the spot on the WFS. The LBWFS, however, has 16×16 pixels with a plate scale of $0.146''$ per pixel, so the spot is oversampled and the centroid is independent of the spot size.

Slowly-varying LGS aberrations are detected as the difference between the NGS wavefront measured by the LBWFS and the time-average of the LGS wavefront measured by the WFS. Focus is compensated by moving the wavefront sensor stage to keep the wavefront sensor conjugate to the LGS [7], while the higher-order aberrations are compensated by changing the reference centroids for the fast WFS [5]. The difference between the measured centroids and the reference centroids is fed to the wavefront reconstructor to drive the actuators of the deformable mirror. If the tip-tilt NGS has a visual magnitude of 17 or brighter, these aberrations can be measured with the LBWFS and corrected. However, if the NGS is fainter or if the telescope pupil is rotating rapidly on the LBWFS, it is not possible to measure and adequately compensate for these aberrations. Hence, a model is needed for how these aberrations change with pupil angle in order to correct them without explicitly measuring them. The aim of this investigation was initially to derive such a model and implement it on the sky. It was found that an empirically derived model works well on the same night that the data used to generate the model was taken. However, since the magnitude of the LGS aberrations, which can be as high as 1000 nm RMS, changes from night to night, it has not been possible to compensate for them using exclusively prior knowledge.

#68578 - $15.00 USD Received 2 March 2006; revised 11 April 2006; accepted 11 April 2006

In Sect. 2, we describe sources of the LGS aberrations while on-sky measurements and a model to explain them are presented in Sect. 3. Section 4 concludes the paper with a discussion of the implications of the LGS aberrations.

2. Sources of LGS aberrations

In this section we postulate and describe four sources of LGS aberrations. Since we do not completely understand the aberrations that we measure, there are likely to be other sources as well.

2.1. Asymmetric spot elongation

The physical LGS spot on the sky is located at a finite height, $h \approx 90$ km, and has a finite thickness, t, ranging between 10 km and 20 km. The spot as seen by each subaperture appears elongated due to a parallax effect. Since every subaperture looks at the laser spot from a different angle, the elongation in each subaperture is different. The elongation of the spot increases with increasing baseline, b, between the launch telescope and the subaperture. To first order, the elongation, η, is given by

$$\eta = \cos(\zeta) bt/h^2, \tag{1}$$

where ζ is the zenith angle.

If the elongation were symmetrical one would not expect it to introduce any aberrations. However, the sodium density profile has a time-varying structure and is not symmetrical. In addition, the parallax effect itself is asymmetric. Since the elongation is proportional to h^{-2}, the bottom part of the sodium layer appears more elongated than the top. For example, the part of the LGS spot located at 80 km appears to be 1.56 times as elongated than the part at 100 km. Thus, the spot elongation process is asymmetric, with a longer tail pointing towards the ground.

We measure the spot elongation in the following manner. The primary mirror of the Keck II telescope is comprised of 36 hexagonal segments. By applying focus to each segment, 36 distinct images can be formed in the telescope focal plane. In this way, the AO acquisition camera can be used to record images of the laser guide star viewed from different vantage points in the telescope pupil in a single exposure (Fig. 1). The spot elongation can be seen to increase with distance from the projection telescope, located to the right of the telescope primary in these images.

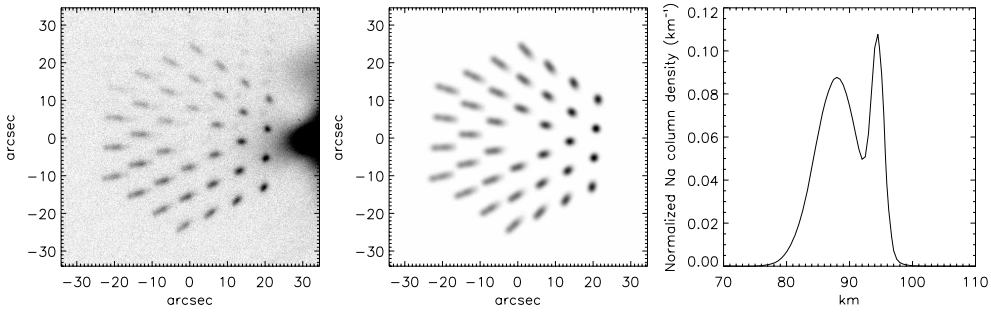

Fig. 1. Images of the LGS on January 26, 2005, formed by adding focus across the primary mirror segments (left), and a corresponding simulated image (center) using an estimated sodium profile (right). The launch telescope is located to the right of the pupil, where the Rayleigh scatter can be seen.

It is possible to deduce the structure of the sodium layer present at the time of such an image. We model the laser as a cylindrical beam 50 cm diameter, exciting a sodium layer with an

#68578 - $15.00 USD Received 2 March 2006; revised 11 April 2006; accepted 11 April 2006

arbitrary stratified density structure. The image formed by each of the 36 segments is computed separately by tracing a ray at the center of each imaging pixel through the atmosphere, and integrating the sodium density encountered in the illuminated cylinder. The 36 images are then convolved by the seeing estimate and superimposed, and parameters of the model optimized to match the observed image.

On many nights, the vertical sodium density can be adequately modeled as the sum of two Gaussian functions, as shown in the right panel of Fig. 1. On this particular night, the Gaussians were centered at heights 88 km and 94.5 km, with standard deviations of 3.5 km and 1 km respectively. Finer structure is not apparent in these images, taken in 1.1" seeing.

2.2. Bias due to quad-cell centroid

If the spot on the WFS is well sampled, then the centroid is, by definition, nulled when the center-of-mass of the spot coincides with the center of the subaperture. For a quad cell, the centroid estimates is equal to zero when the intensity to the left of the cross-hairs is the same as the intensity to the right, and the intensity to the above the cross-hairs is the same as the intensity below. For symmetric spots, these two centroids yield the same result regardless of the sampling. However, for asymmetric spots, the center-of-mass centroid does not coincide with the quad cell centroid. Hence, there is a bias in the centroid when quad cells are used which increases as the distance between the laser and the subaperture increases.

The bias also depends on the angle between the direction of spot elongation and the alignment of the quad cells. When the position of the laser is perfectly aligned with the quad cells, the bias is at its greatest; when the the spot elongation is at 45° from the quad cells, the bias is at its smallest.

2.3. Bias due to truncation of spot

If the spot on the WFS is not symmetric, truncation of the spot introduces another bias. There are two sources of truncation: a circular field stop with a radius of $2.4''$ located at the focus of the telescope in front of the WFS by the $2.4''$ angular extent of each pixel. The resulting biases have two components: one with circular symmetry and one with rectangular symmetry in the direction of the pixels.

2.4. Telescope and AO system aberrations

Because the LGS is situated at a height of about 90 km, the focal plane of the LGS differs from the focal plane of the NGS. In LGS AO, the telescope stays focused at infinity and the stage carrying the WFS moves to cancel the focus error seen by the WFS. A Zemax model shows that the on-axis wavefront error introduced by imaging the LGS due to the telescope is only 5 nm. This is contrast with the formula presented in Ragazzoni,[8] which predicts about 39 nm of spherical aberration. A Zemax model of the AO system with the LGS at infinity and the WFS refocused shows 9 nm of spherical aberration and 122 nm of x-coma.

3. Measuring and modeling the aberrations

The aberrations were measured on the sky using dedicated telescope time. The measurement was performed in the following way. The tip-tilt loop was locked on a 10^{th} magnitude NGS and the deformable mirror loop was locked on the LGS, with the reference centroids set to be all zeros. The rotator mode was selected to keep the pupil fixed on both the WFS and the LBWFS, and three images were taken with the LBWFS. Then the pupil angle was rotated by 360° in 30° increments and LBWFS images were captured at each pupil angle. As the pupil angle changes, the position of the laser relative to the pupil changes. The laser is located

#68578 - $15.00 USD Received 2 March 2006; revised 11 April 2006; accepted 11 April 2006

at the top of the pupil for a pupil angle of 116.6°. The first 11 Zernike coefficients[9] were computed using a least-squares fit of the Zernike derivatives to the centroids of the images. The results using measurements taken near zenith are plotted in Fig. 2 for the astigmatism, coma and spherical aberration terms. We can model the first three contributors to the LGS aberrations

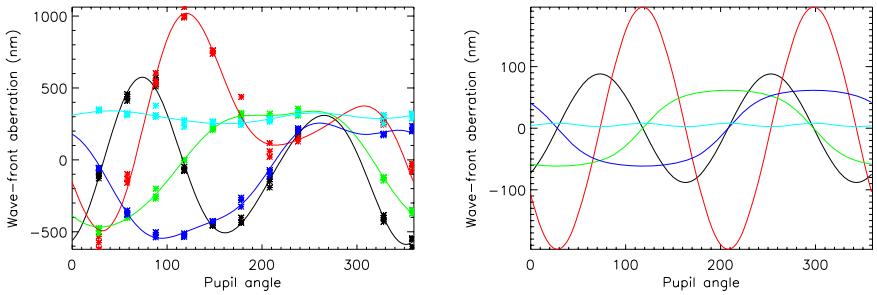

Fig. 2. The measured (left) and modeled (right) LGS aberrations as a function of pupil angle near zenith. The curves are, 0° astigmatism (red), 45° astigmatism (black), spherical aberration (light blue), *y*-coma (green) and *x*-coma (dark blue).

in Sect. 2 as stemming from a bias in the centroids. This bias has two components: a circularly symmetric component which is a function of the distance, $r = \sqrt{x^2+y^2}$, between the laser and the subaperture, and a rectangular component in x which is a function of the distance (in meters) along the x-axis from the center of the telescope (and the same for y). We can write the centroid bias as the product of two arbitrary functions, f and g:

$$s_x = f(x)g(r) \tag{2}$$

and

$$s_y = f(y)g(r). \tag{3}$$

We found that by writing the functions in the form:

$$s_x = \text{signum}(x)|x|^{\alpha} r^{\beta} \tag{4}$$

$$s_y = \text{signum}(y)|y|^{\alpha} r^{\beta}, \tag{5}$$

and fitting the parameters α and β, we could obtain a reasonable fit to the data for different elevations and sodium density profiles. The modeled aberrations as a function of pupil angle are plotted in Fig. 2 with $\alpha = 1.55$ and $\beta = 1.95$ and the absolute magnitude chosen to that the model matches the appearance the measured aberrations. However, there are two discrepancies that need to be investigated further: why the strength of the measured astigmatism is larger for pupil angles in the range $[0°, 180°]$ and why the measured astigmatism and coma terms all have a non-zero mean.

At larger zenith angles, the aberrations take a similar form but have a smaller amplitude. The value of the astigmatism and coma terms averaged over all pupil angles is also smaller.

4. Conclusion and discussion

LGS AO systems experience aberrations due to biases in the centroids. The biases are caused by WFS spot elongation, by using quad cells and by the truncation of the WFS spot. There are also aberrations introduced by the optics of the telescope and AO system, since both optical systems are optimized for an object at infinity. The wavefront error due to the aberrations is extremely

#68578 - $15.00 USD Received 2 March 2006; revised 11 April 2006; accepted 11 April 2006

large and, if uncorrected, is larger than all the other wavefront error terms combined.[5] Hence, it is essential that these aberrations be measured and corrected, and future LGS AO systems should include a LBWFS for this purpose. To reduce the effects of the LGS aberrations, we intend to launch the LGS behind the secondary when we upgrade the Keck I telescope's AO system to include LGS AO capabilities. We are also upgrading the WFSs on both telescopes to have 8×8 pixels per subaperture in LGS AO mode. Future work will include a rigorous model of the effect of spot elongation on the wavefront sensor, investigations into other telescope diameters and laser projection geometries and ways to mitigate and measure more efficiently the LGS aberrations. This will help understand how extremely large telescopes with multiple LGSs will be affected by these LGS aberrations.

Acknowledgments

The data presented herein were obtained at the W. M. Keck Observatory, which is operated as a scientific partnership among the California Institute of Technology, the University of California, and the National Aeronautics and Space Administration. The Observatory was made possible by the generous financial support of the W. M. Keck Foundation. The authors wish to recognize and acknowledge the significant cultural role and reverence that the summit of Mauna Kea has always had within the Hawaiian community. We are most fortunate to have the opportunity to conduct observations from this mountain. This work has been supported by the National Science Foundation Science and Technology Center for Adaptive Optics, managed by the University of California at Santa Cruz under cooperative agreement No. AST - 9876783.

#68578 - $15.00 USD Received 2 March 2006; revised 11 April 2006; accepted 11 April 2006